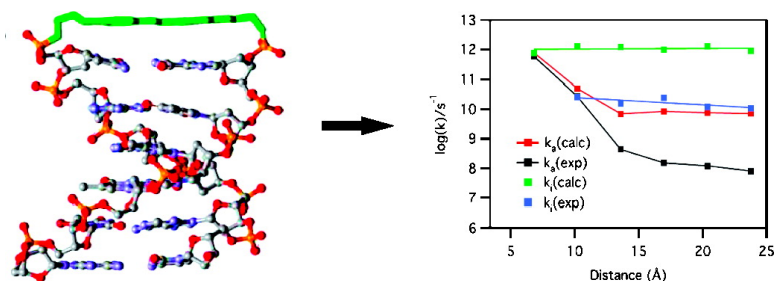


## Effect of Structural Dynamics on Charge Transfer in DNA Hairpins

Ferdinand C. Grozema, Stefano Tonzani, Yuri A. Berlin, George C. Schatz, Laurens D. A. Siebbeles, and Mark A. Ratner

*J. Am. Chem. Soc.*, **2008**, 130 (15), 5157-5166 • DOI: 10.1021/ja078162j • Publication Date (Web): 07 March 2008

Downloaded from <http://pubs.acs.org> on February 8, 2009



### More About This Article

Additional resources and features associated with this article are available within the HTML version:

- Supporting Information
- Links to the 5 articles that cite this article, as of the time of this article download
- Access to high resolution figures
- Links to articles and content related to this article
- Copyright permission to reproduce figures and/or text from this article

[View the Full Text HTML](#)

## Effect of Structural Dynamics on Charge Transfer in DNA Hairpins

Ferdinand C. Grozema,<sup>\*,†,‡</sup> Stefano Tonzani,<sup>‡</sup> Yuri A. Berlin,<sup>‡</sup> George C. Schatz,<sup>‡</sup>  
Laurens D. A. Siebbeles,<sup>†</sup> and Mark A. Ratner<sup>‡</sup>

*Opto-electronic Materials Section, DelftChemTech, Delft University of Technology, Julianalaan 136, 2628 BL, Delft, The Netherlands, and Center for Nanofabrication and Molecular Self-Assembly, Department of Chemistry, Northwestern University, 2145 Sheridan Road, Evanston, Illinois 60208-3113*

Received October 25, 2007; E-mail: f.c.grozema@tudelft.nl

**Abstract:** We present a theoretical study of the positive charge transfer in stilbene-linked DNA hairpins containing only AT base pairs using a tight-binding model that includes a description of structural fluctuations. The parameters are the charge transfer integral between neighboring units and the site energies. Fluctuations in these parameters were studied by a combination of molecular dynamics simulations of the structural dynamics and density functional theory calculations of charge transfer integrals and orbital energies. The fluctuations in both parameters were found to be substantial and to occur on subpicosecond time scales. Tight-binding calculations of the dynamics of charge transfer show that for short DNA hairpins (<4 base pairs) the charge moves by a single-step superexchange mechanism with a relatively strong distance dependence. For longer hairpins, a crossover to a fluctuation-assisted incoherent mechanism was found. Analysis of the charge distribution during the charge transfer process indicates that for longer bridges substantial charge density builds up on the bridge, but this charge density is mostly confined to the adenine next to the hole donor. This is caused by the electrostatic interaction between the hole on the AT bridge and the negative charge on the hole donor. We conclude both that the relatively strong distance dependence for short bridges is mostly due to this electrostatic interaction and that structural fluctuations play a critical role in the charge transfer, especially for longer bridge lengths.

### Introduction

The dynamics and mechanism of charge transfer through DNA have been subjects of considerable debate over the last two decades. Despite the large amount of work done in this area, it still attracts the attention of both theoreticians and experimentalists.<sup>1–3</sup> Initially, the photoinduced charge transfer in donor–DNA–acceptor systems was mostly discussed in terms of a single-step superexchange mechanism in which the charge tunnels from the donor to the acceptor without actually becoming localized on the bridge. This mechanism generally gives rise to an exponential distance dependence of the charge transfer rate,  $k_{CT}$ , according to<sup>4–6</sup>

$$k_{CT} = k_0 e^{-\beta R} \quad (1)$$

where  $R$  is the distance between donor and acceptor,  $\beta$  is the falloff parameter, and  $k_0$  is a scaling factor. In the superexchange

mechanism, the value of  $\beta$  is typically larger than  $0.3 \text{ \AA}^{-1}$ . In the case of hole transfer through DNA, values as small as  $0.1 \text{ \AA}^{-1}$  have also been reported.<sup>7–9</sup> For such small values, the rate hardly depends on the distance, and another mechanism, incoherent hopping, is believed to be operative.<sup>10–12</sup> It is well-established that, for hole transfer in DNA sequences containing both guanine–cytosine (GC) and adenine–thymine (AT) base pairs, the transfer predominantly takes place by hopping between the guanine bases.<sup>10–15</sup> The nature of these individual hopping steps is still under debate. For short bridges of up to 3 AT base pairs between GCs, the mechanism is most likely to be single-step superexchange since in most experimental data relatively high  $\beta$  values have been found for these bridge lengths.<sup>16–21</sup>

(7) Murphy, C. J.; Arkin, M. R.; Jenkins, Y.; Ghatlia, N. D.; Bossmann, S. H.; Turro, N. J.; Barton, J. K. *Science* **1993**, *262*, 1025–1029.

(8) Hall, D. B.; Holmlin, E.; Barton, J. K. *Nature* **1996**, *382*, 731–735.

(9) Henderson, P. T.; Jones, D.; Hampikian, G.; Kan, Y.; Schuster, G. B. *Proc. Natl. Acad. Sci. U.S.A.* **1999**, *96*, 8353–8358.

(10) Berlin, Y.; Burin, A. L.; Ratner, M. A. *J. Phys. Chem. A* **1999**, *104*, 443–445.

(11) Berlin, Y. A.; Burin, A. L.; Ratner, M. A. *J. Am. Chem. Soc.* **2001**, *123*, 260–268.

(12) Bixon, M.; Giese, B.; Wessely, S.; Langenbacher, T.; Michel-Beyerle, M. E.; Jortner, J. *Proc. Natl. Acad. Sci. U.S.A.* **1999**, *96*, 11713–11716.

(13) Giese, B.; Wessely, S.; Spormann, M.; Lindemann, U.; Meggers, E.; Michel-Beyerle, M. E. *Angew. Chem., Int. Ed.* **1999**, *38*, 996–996.

(14) Giese, B. *Acc. Chem. Res.* **2000**, *33*, 631–636.

(15) Giese, B. *Top. Curr. Chem.* **2004**, *236*, 27–44.

(16) Brun, A. M.; Harriman, A. *J. Am. Chem. Soc.* **1994**, *116*, 10383–10393.

<sup>†</sup> Delft University of Technology.

<sup>‡</sup> Northwestern University.

(1) Schuster, G. B., Ed. *Long-range charge transfer in DNA*; Springer-Verlag: Berlin, 2004.

(2) Wagenknecht, H.-A., Ed. *Charge transfer in DNA*; Wiley-VCH: Weinheim, Germany, 2005.

(3) Chakraborty, T., Ed. *Charge migration in DNA*; Springer: Berlin, 2007.

(4) Bixon, M.; Jortner, J. *Adv. Chem. Phys.* **1999**, *106*, 35–202.

(5) Schatz, G. C.; Ratner, M. A. *Quantum Mechanics in Chemistry*; Dover Publications: Mineola, NY, 2002.

(6) Priyadarshy, S.; Risser, S. M.; Beratan, D. N. *J. Phys. Chem.* **1996**, *100*, 17678–17678.

For longer bridges ( $>3$  ATs), the mechanism appears to cross over to hopping on the AT bridge since it has been shown that the dependence of the hole transfer rate on the distance is much weaker in this case.<sup>22–24</sup>

Recently, a similar flattening of the distance dependence at long AT bridge lengths, as observed in the case of a  $G^+$  donor, was found for hole transfer in stilbene-linked DNA hairpins in which a photoexcited stilbene derivative is the donor.<sup>25,26</sup> In this case, the explanation may be somewhat more complicated since the electrostatic potential of the negative charge on the photoexcited donor that stays behind after charge separation can have a significant effect on the motion of the positive charge to the acceptor. Moreover, the distance dependence of charge transfer in DNA hairpins (or the value of  $\beta$ ) has been shown to depend strongly on the injection energy, the energy difference between a hole localized on the donor and a hole localized on a bridge site.<sup>27</sup>

Fiebig and co-workers have reported that, in a system where photoexcited ethidium is the hole donor, the charge transfer rate either can be independent of distance<sup>28</sup> or exhibits very strong distance dependence,<sup>29</sup> depending on the way in which the ethidium moiety intercalates in the DNA stack. This indicates that also the precise orientation of the donor and acceptor with respect to the DNA bases influences the distance dependence that is observed.<sup>29</sup>

The very different distance dependencies of the charge transfer rate in these two regimes signify that different mechanisms of charge transfer must be operative.<sup>30</sup> For the regime with strong exponentially decaying distance dependence, this mechanism is single-step superexchange. The value of  $\beta$  in this case depends strongly on the relative magnitude of the injection energy and the charge transfer integrals between neighboring units in the system.<sup>23,27,31,32</sup> If the injection energy is large compared to the charge transfer integrals, a strong dependence of the charge transfer rate on distance will be observed. If the magnitude of the injection energy becomes comparable to

the charge transfer integrals, low values of  $\beta$  will be obtained. In this case, it is more likely that the charge populates the bridge or even becomes localized there. This leads to a transition from single-step superexchange to an incoherent mechanism, either hopping of localized charges<sup>10–12,33</sup> or polaron diffusive motion.<sup>9,34,35</sup> A crossover between the regimes of superexchange tunneling and incoherent motion will be observed in systems with an injection energy larger than the electronic coupling between nearest neighbors. For short distances, the superexchange rate is large but decreases rapidly with distance. At a certain bridge length, it becomes more favorable to inject a charge into the bridge, leading to incoherent transport with weak distance dependence. Bixon et al.<sup>24</sup> and Berlin et al.<sup>23</sup> have shown that these two models can be combined to describe the experimentally observed crossover from strong to weak distance dependence in DNA.

Two important parameters that determine the mechanism of charge transfer in DNA are the site energies (the energy of a charge when localized on a single unit) and the charge transfer integrals. Both of these parameters critically depend on geometric fluctuations in DNA, and therefore, the hole transfer rate is strongly coupled to fluctuations in the DNA structure. Several authors have noted the important role of structural fluctuations in the mechanism of charge transport through DNA,<sup>29,36–42</sup> but none have explicitly studied the effect of fluctuations on the mechanism of hole transfer through DNA.

In this paper, we describe a detailed theoretical study of the magnitude of fluctuations in the energies and charge transfer integrals along the donor–DNA–acceptor system, and we examine the consequences of these fluctuations for the mechanism of hole transfer. We have chosen the series of stilbene-capped DNA hairpins recently studied by Lewis et al. (see Figure 1) since these are relatively small and experiments have indicated that both the superexchange and hopping regimes are operative in these systems.<sup>25,26</sup> We have used molecular dynamics simulations and density functional theory calculations to study the magnitude and time scale of fluctuations in the site energies and charge transfer integrals in DNA hairpins. These data were used in tight-binding calculations to evaluate the effects of these fluctuations on hole transfer in the hairpins. We show that the energy barrier is much higher than the average values of the charge transfer integrals. However, the fluctuations in the site energies and charge transfer integrals are sufficiently large to lead to a fluctuation-assisted incoherent transport mechanism for longer hairpins. It is also shown that the inclusion of the electrostatic interaction between the hole and the negative charge that remains on the hole donor is essential to obtain a regime with strong distance dependence at short donor–acceptor separation.

- (17) Fukui, K.; Tanaka, K. *Angew. Chem., Int. Ed.* **1998**, *37*, 158–161.  
 (18) Meade, T. J.; Kayyem, J. F. *Angew. Chem., Int. Ed. Engl.* **1995**, *34*, 352–354.  
 (19) Lewis, F. D.; Liu, X.; Wu, Y.; Miller, S. E.; Wasielewski, M. R.; Letsinger, R. L.; Sanishvili, R.; Joachimiak, A.; Tereshko, V.; Egli, M. *J. Am. Chem. Soc.* **1999**, *121*, 9905–9906.  
 (20) Meggers, E.; Michel-Beyerle, M. E.; Giese, B. *J. Am. Chem. Soc.* **1998**, *120*, 12950–12955.  
 (21) Lewis, F. D.; Liu, X.; Liu, J.; Miller, S. E.; Hayes, R. T.; Wasielewski, M. R. *Nature* **2000**, *406*, 51–53.  
 (22) Giese, B.; Amaudrut, J.; Kohler, A.-K.; Spormann, M.; Wessely, S. *Nature* **2001**, *412*, 318–320.  
 (23) Berlin, Y. A.; Burin, A. L.; Ratner, M. A. *Chem. Phys.* **2002**, *275*, 61–74.  
 (24) Bixon, M.; Jortner, J. *Chem. Phys.* **2002**, *281*, 393–408.  
 (25) Lewis, F. D.; Zhu, H.; Daublain, P.; Cohen, B.; Wasielewski, M. R. *Angew. Chem., Int. Ed.* **2006**, *45*, 7982–7985.  
 (26) Lewis, F. D.; Zhu, H.; Daublain, P.; Fiebig, T.; Raytchev, M.; Wang, Q.; Shafirovich, V. *J. Am. Chem. Soc.* **2006**, *128*, 791–800.  
 (27) Lewis, F. D.; Liu, J.; Weigel, W.; Rettig, W.; Kurnikov, I. V.; Beratan, D. N. *Proc. Natl. Acad. Sci. U.S.A.* **2002**, *99*, 12536–12541.  
 (28) Wan, C.; Fiebig, T.; Kelley, S. O.; Treadway, C. R.; Barton, J. K.; Zewail, A. H. *Proc. Natl. Acad. Sci. U.S.A.* **1999**, *96*, 6014–6019.  
 (29) Valis, L.; Wang, Q.; Raytchev, M.; Buchvarov, I.; Wagenknecht, H.-A.; Fiebig, T. *Proc. Natl. Acad. Sci. U.S.A.* **2006**, *103*, 10192–10195.  
 (30) Berlin, Y. A.; Kurnikov, I. V.; Beratan, D.; Ratner, M. A.; Burin, A. L. *Top. Curr. Chem.* **2004**, *237*, 1–36.  
 (31) Lewis, F. D.; Wasielewski, M. R. Dynamics of photoinitiated hole and electron injection in duplex DNA. In *Charge transfer in DNA*; Wagenknecht, H.-A., Ed.; Wiley-VCH: Weinheim, Germany, 2005; pp 93–116.  
 (32) Grozema, F. C.; Berlin, Y. A.; Siebbeles, L. D. A. *J. Am. Chem. Soc.* **2000**, *122*, 10903–10909.

- (33) Bixon, M.; Jortner, J. *J. Am. Chem. Soc.* **2001**, *123*, 12556–12567.  
 (34) Conwell, E. M.; Bloch, S. M.; McLaughlin, P. M.; Basko, D. M. *J. Am. Chem. Soc.* **2007**, *129*, 9175–9181.  
 (35) Conwell, E. M.; Rakhmanova, S. V. *Proc. Natl. Acad. Sci. U.S.A.* **2000**, *97*, 4556–4560.  
 (36) Schuster, G. B. *Acc. Chem. Res.* **2000**, *33*, 253–260.  
 (37) O’Neil, M. A.; Barton, J. K. *J. Am. Chem. Soc.* **2004**, *126*, 11471–11483.  
 (38) O’Neil, M. A.; Barton, J. K. *J. Am. Chem. Soc.* **2004**, *126*, 13234–13235.  
 (39) Voityuk, A. A.; Siritwong, K.; Rösch, N. *Phys. Chem. Chem. Phys.* **2001**, *3*, 5421–5425.  
 (40) Troisi, A.; Orlandi, G. *J. Phys. Chem. B* **2002**, *106*, 2093–2101.  
 (41) Grozema, F. C.; Siebbeles, L. D. A.; Berlin, Y. A.; Ratner, M. A. *ChemPhysChem* **2002**, *3*, 536–539.  
 (42) Troisi, A.; Ratner, M.; Zimmt, M. B. *J. Am. Chem. Soc.* **2004**, *126*, 2215–2224.

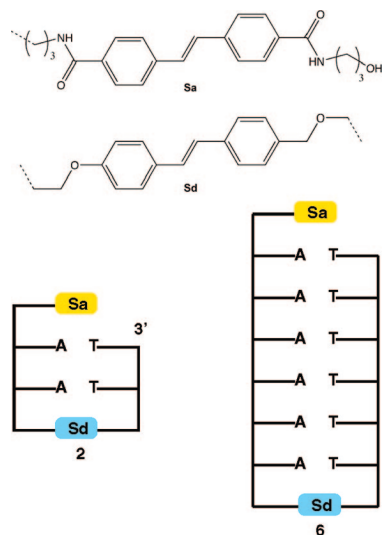


**Figure 1.** Schematic representation of the stilbene-linked DNA hairpins **2** and **6** (bottom) and the chemical structure of the stilbene linker, **Sd**, and stilbene cap, **Sa** (top). The number labeling the hairpins corresponds to the number of adenine–thymine base pairs present.

The key difference between our present work and previous theoretical explanations for the change in distance dependence of the charge transfer rate as the length of the DNA bridge increases is that we do not make a priori assumptions about a change in mechanism (from superexchange to hopping) as was done in earlier theoretical work.<sup>23,43</sup> We have used a single tight-binding model with accurately calculated parameters to describe the charge transfer for all donor–bridge–acceptor distances. We show that the calculated results are in good qualitative agreement with the full range of experimental data for these hairpins.

### Computational Methodology

Two of the important parameters that determine the rate of charge transfer between two neighboring bases are the site energy (the energy difference for a charge localized on one base or the other) and the charge transfer integral between the neighboring bases. To describe the motion of charges from a donor to an acceptor through a DNA bridge, a whole sequence of charge transfer reactions along several nucleobases has to be considered. Each of these charge transfer reactions is characterized by a specific charge transfer integral and energy difference, which both depend on the orientation of the bases with respect to each other, the geometry of the nucleobase itself, and on the local environment (e.g., the presence of counterions or the water surrounding the DNA). To study the transfer of charges through a DNA bridge, we use a tight-binding model, which can take these variations in the energy difference and charge transfer integral along the DNA double helix into account.<sup>32,41,44</sup> The wave function of the charge,  $\Psi(t)$ , is taken to be a linear combination of basis functions,  $\varphi_n$ , that are localized on each nucleobase, with expansion coefficients  $c_n$ .

$$\Psi(t) = \sum_{n=1}^N c_n(t) |\varphi_n\rangle \quad (2)$$

In the case of the migration of positive charges through DNA, the wave function of the charge can, to a good approximation, be expressed as a linear combination of the highest occupied molecular orbitals (HOMO) of the individual nucleobases. In typical experi-

ments on donor–DNA–acceptor systems, a hole is usually created on the hole donor, for example, by photoexcitation, and can be considered localized initially. This initial condition is satisfied in our simulations by setting the expansion coefficient on the donor site equal to one at  $t = 0$ , while all others are taken to be zero. The motion of the charge along the DNA bridge toward the acceptor is simulated by propagating the wave function in time according to the time-dependent Schrödinger equation.

$$i\hbar \frac{\partial \Psi(t)}{\partial t} = \hat{H} \Psi(t) \quad (3)$$

The exact way in which the wave function evolves with time is determined by the Hamiltonian matrix (eq 4). The diagonal matrix elements of this matrix correspond to the site energies,  $\epsilon_{ii} = \langle \varphi_i | \hat{H} | \varphi_i \rangle$ , that is, the energy of a charge carrier when it is localized on a single nucleobase (or the donor and acceptor). In the simplest approximation, the site energies correspond to the ionization potential of a single nucleobase (as well as the donor and the acceptor) in the case of transfer of positive charges. However, it is important to note that the site energy can change considerably depending on the neighboring bases.<sup>45,46</sup>

When only nearest neighbor interactions are taken into account, the off-diagonal matrix elements of the Hamiltonian are equal to the electronic coupling,  $V_{ij} = \langle \varphi_i | \hat{H} | \varphi_j \rangle$ , between the HOMO orbitals on adjacent nucleobases, while all other off-diagonal matrix elements are zero. The Hamiltonian matrix is then given by

$$H = \begin{pmatrix} \epsilon_{11} & V_{12} & 0 & K & 0 \\ V_{21} & \epsilon_{22} & & & \\ 0 & \dots & & & \\ M & & \dots & & \\ 0 & & & & \epsilon_{NN} - \frac{i\hbar}{\tau} \end{pmatrix} \quad (4)$$

In order to ensure that the charge is irreversibly trapped when it arrives on the acceptor, a complex part is added to the diagonal matrix element of the acceptor site ( $N$ ),  $H_{NN} = \epsilon_{NN} - i\hbar/\tau$ . A decay time  $\tau$  of 1 fs was used in the simulations described here. The value of  $\tau$  was chosen to be small enough that the charge disappears from the last site instantaneously but not so small to cause reflections of the wave function on the last site. Variation of  $\tau$  by a factor of 2 was not found to influence the results. The irreversible decay of the hole at the acceptor site leads to a decay of the total charge density on the donor–DNA–acceptor system.

The decay of the charge on the acceptor site leads to an overall decay of the amount of charge present, the so-called survival probability,  $P(t)$ . Experimentally, the rate of charge arrival at the acceptor defines the charge transfer rate, and therefore, the decay of  $P(t)$  corresponds to the formation of the charge-separated state. In our tight-binding description, the survival probability is defined as

$$P(t) = \sum_n^N |c_n(t)|^2 \quad (5)$$

The rate of arrival of the charge at the acceptor site,  $k_a$ , can be obtained from the decay of the survival probability in time since the charge decays very rapidly at the last site. This arrival rate is equivalent to the charge transfer rate,  $k_{CT}$ , defined in eq 1. It should be noted  $k_{CT}$  is sometimes used in experimental work to indicate the rate at which the hole leaves the hole donor, assuming single-step charge transfer. Since the charge transfer does not necessarily occur in a single-step,  $k_{CT}$  is not always the same as the rate at which the charge leaves the donor.<sup>25</sup>

(43) Bixon, M.; Jortner, J. *Chem. Phys.* **2002**, *281*, 393–408.

(44) Grozema, F. C.; Berlin, Y. A.; Siebbeles, L. D. A. *Int. J. Quantum Chem.* **1999**, *75*, 1009–1016.

(45) Voityuk, A. A.; Jortner, J.; Bixon, M.; Rösch, N. *Chem. Phys. Lett.* **2000**, *324*, 430–434.

(46) Senthilkumar, K.; Grozema, F. C.; Fonseca Guerra, C.; Bickelhaupt, F. M.; Siebbeles, L. D. A. *J. Am. Chem. Soc.* **2003**, *125*, 13658–13659.

Both the site energies and the charge transfer integrals in eq 4 are sensitive to the geometry of the DNA. In our previous work, we considered the effect of small fluctuations in  $V$  from its average value corresponding to the equilibrium B-DNA structure.<sup>41,47</sup> In these calculations, we only took fluctuations in the twist angle between neighboring bases into account. These calculations demonstrated that even such small fluctuations have a considerable effect on the charge transfer rates<sup>47</sup> and charge carrier mobility in DNA.<sup>41</sup> In reality, the structural fluctuations can be expected to be much stronger due to variations in many other degrees of freedom, for example, the stacking distance (rise), the shift, the tilt, etc. Recently, it was shown that the value of the charge transfer integral is indeed very sensitive to dynamic fluctuations in these degrees of freedom.<sup>48</sup> Additionally, variations of the geometry inside the individual bases can also influence the charge transfer integrals between neighboring bases.

In this work, we consider all possible geometry changes that give rise to fluctuations in  $\epsilon$  and  $V$  by performing atomistic molecular dynamics (MD) simulations of the DNA hairpins in solution. For the hairpin structures obtained from these simulations, the distributions of  $\epsilon$  and  $V$  were obtained and also information on the time scale of the fluctuations was deduced. The information obtained from MD simulations is used in the tight-binding calculations of the charge transfer kinetics by including fluctuations in  $\epsilon$  and  $V$  on a certain time scale, as will be discussed below. We have performed classical MD simulations of two of the hairpins (**2** and **6**) in solution at 300 K, using the Amber 8 package,<sup>49</sup> similar to the simulations described previously.<sup>50</sup> The details of the MD simulations are given in the Supporting Information.

As mentioned above, the wave function for a positive charge in DNA hairpins can be expressed as a linear combination of the HOMOs on the individual units (the adenine or the stilbene donor/acceptor). The charge transfer integrals between the HOMOs on neighboring units were calculated directly by density functional theory (DFT) using the fragment orbital approach in the Amsterdam density functional program (ADF).<sup>51</sup> In this approach, a DFT calculation is performed for a dimer of two units in which the orbitals of the dimer are expressed as a linear combination of the molecular orbitals of the individual units. In this way, the charge transfer integral,  $V$ , is directly obtained as the off-diagonal matrix element of the Kohn–Sham Hamiltonian matrix.<sup>52</sup> The values of the effective charge transfer integral  $V^{\text{eff}}$  account for the nonzero overlap between the HOMOs on neighboring bases and are used in the present work.<sup>52</sup> The DFT calculations for the individual bases were performed using an atomic basis set of Slater-type orbitals of double- $\zeta$  quality including polarization functions (TZP basis set).<sup>53</sup> All calculations were performed using the asymptotically correct statistical average of orbital potentials (SAOP) model functional.<sup>54</sup>

## Results and Discussion

We consider hole transfer in a series of stilbene-linked DNA hairpins of increasing length that are capped with another

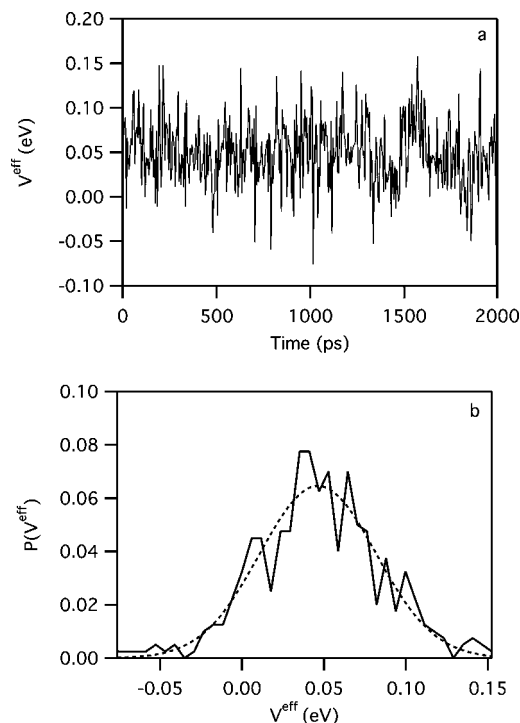


**Figure 2.** (a) Value of  $V^{\text{eff}}$  between the two adenines in hairpin **2** as a function of time. (b) Probability distribution of the values of  $V^{\text{eff}}$ .

stilbene derivative. The stilbenediether (**Sd**) linker that acts as a hole acceptor is connected to both DNA strands, while the capping stilbenedicarboxamide (**Sa**) that acts as the hole donor is connected to only one strand. The DNA in these systems consists only of adenine–thymine (AT) base pairs. Examples of the hairpins that we studied here are shown in Figure 1. Lewis and co-workers have extensively studied photoinduced hole transfer in such hairpins.<sup>25,26,31,55</sup> In these experiments, selective photoexcitation of **Sa** ultimately leads to full charge separation, resulting in a negatively charged **Sa** and a positively charged **Sd**. The most recent experiments of Lewis et al. not only monitored the decay of the excited state of the donor (**Sa**<sup>\*</sup>) but also allowed the direct observation of the formation of the acceptor radical cation (**Sd**<sup>+</sup>).<sup>25,26</sup>

We have performed MD simulations for hairpins **1** and **6** of the type shown in Figure 1. From these MD simulations, an ensemble of structures was obtained for which the charge transfer integrals and energetics were evaluated.

**1. Fluctuations in the Charge Transfer Integrals.** The effective charge transfer integrals between neighboring units (stilbene or DNA base) were calculated for 400 snapshots from a 2 ns MD simulation of a DNA hairpin containing two AT base pairs (hairpin **2**) using the fragment orbital method described above. The effective charge transfer integral between the adenine bases is shown in Figure 2a as a function of time. The value of  $V^{\text{eff}}$  strongly fluctuates around an average value close to 0.05 eV. The distribution of  $V^{\text{eff}}$  for the 400 conformations considered is shown in Figure 2b and is close to Gaussian. The fitted Gaussian in Figure 2b is centered on an average value of 0.046 eV and has a mean square deviation of 0.05 eV. Clearly, the variations in  $V^{\text{eff}}$  are of the same order of magnitude as the average value, which emphasizes the importance of

(47) Senthilkumar, K.; Grozema, F. C.; Fonseca Guerra, C.; Bickelhaupt, F. M.; Lewis, F. D.; Berlin, Y. A.; Ratner, M. A.; Siebbeles, L. D. A. *J. Am. Chem. Soc.* **2005**, *127*, 14894–14903.

(48) Sadowska-Aleksiejew, A.; Rak, J.; Voityuk, A. A. *Chem. Phys. Lett.* **2006**, *429*, 546–550.

(49) Cornell, W. D.; Cieplak, P.; Bayly, C. I.; Gould, I. R.; Merz, K. M.; Ferguson, D. M.; Spellmeyer, D. C.; Fox, T.; Caldwell, J. W.; Kollman, P. A. *J. Am. Chem. Soc.* **1996**, *118*, 2309.

(50) Lewis, F. D.; Zhang, L.; Liu, X.; Zuo, X.; Tiede, D. M.; Long, H.; Schatz, G. C. *J. Am. Chem. Soc.* **1996**, *127*, 14445–14453.

(51) te Velde, G.; Bickelhaupt, F. M.; Baerends, E. J.; Fonseca Guerra, C.; van Gisbergen, S. J. A.; Snijders, J. G.; Ziegler, T. *J. Comput. Chem.* **2001**, *22*, 931–967.

(52) Senthilkumar, K.; Grozema, F. C.; Bickelhaupt, F. M.; Siebbeles, L. D. A. *J. Chem. Phys.* **2003**, *119*, 9809–9817.

(53) Snijders, J. G.; Vernooijs, P.; Baerends, E. J. *Atomic Data and Nuclear Data Tables* **1981**, *26*, 483–509.

(54) Chong, D. P.; Gritsenko, O. V.; Baerends, E. J. *J. Chem. Phys.* **2002**, *116*, 1760–1772.

(55) Lewis, F. D.; Wasielewski, M. R. *Top. Curr. Chem.* **2004**, *236*, 45–65.

accounting for dynamic structural fluctuations. Interestingly, the average value of the effective charge transfer integral obtained here is considerably larger than the value obtained previously (0.004 eV) using the same method for a regular B-DNA conformation.<sup>47</sup> This shows that the charge transfer integral for the average structure of the DNA hairpins in solution is quite different from that for the ideal B-DNA conformation, as is suggested by the actual structure of the hairpins.<sup>48</sup>

The large fluctuations found here are consistent with previous calculations by Troisi et al.,<sup>40</sup> who reported similar large variations in the charge transfer integral between neighboring units. The difference between their work and our present calculations is that we also account for geometry fluctuations inside the bases, whereas they kept the geometry of the individual bases fixed.

The DNA conformation in hairpin **2** can be expected to deviate considerably from a regular DNA structure since it contains only 2 base pairs and the presence of the stilbene linker (**Sd**) and cap (**Sa**) can have a significant influence on the geometry. Therefore, we have performed additional MD simulations and calculations of  $V^{\text{eff}}$  for hairpin **6**, containing 6 AT base pairs. In this case, it is expected that the structure is determined more by the DNA part of the hairpin than by the stilbene derivatives.

For the 400 snapshots obtained from this MD simulation, the values of  $V_{34}^{\text{eff}}$  (between the adenines 3 and 4) and  $V_{23}^{\text{eff}}$  were calculated. Both distributions of  $V^{\text{eff}}$  obtained from these calculations were very similar to that shown in Figure 2b for the calculations for hairpin **2**. Although the average values are somewhat different for these two distributions (0.055 eV for adenines 3 and 4, and 0.037 eV for adenines 2 and 3), more statistics would be required to clearly show a difference with the results for hairpin **2**. The widths of the distribution are also very similar. On the basis of these facts, we conclude that the number of base pairs,  $N_{\text{AT}}$ , in the hairpin does not significantly influence the distribution of the values of  $J^{\text{eff}}$  between neighboring adenines if  $N_{\text{AT}} \leq 6$ . We have also compared the values of  $J^{\text{eff}}$  for different combinations of adenines in hairpin **6** and found no correlation between the charge transfer integrals in neighboring dimers; see Supporting Information. This shows that the values of  $V^{\text{eff}}$  to be used in eq 5 for charge transport simulations can be assigned independent of each other. From Figure 2, it is impossible to estimate the time scale on which the fluctuations in  $V^{\text{eff}}$  occur. Additional calculations with a shorter time between the snapshots shows that this time scale is  $\sim 1$  ps; see Supporting Information.

The calculated distributions of  $V^{\text{eff}}$  between the **Sa** hole donor and the neighboring adenine and between the **Sd** hole acceptor and the neighboring adenine for hairpin **2** are given in the Supporting Information. For the charge transfer integral between **Sa** and the first adenine on the bridge, the average value is close to zero (0.005 eV) with a mean square deviation of 0.06 eV. This means that deviations from the average value are essential for charge transfer to occur. The average value of  $V^{\text{eff}}$  between the hole acceptor **Sd** and the last adenine in the bridge is 0.02 eV with a mean square deviation of 0.07 eV.

**2. Energetics of Charge Transfer in DNA Hairpins.** Apart from the charge transfer integrals, the other parameters in the Hamiltonian in eq 5, the site energies,  $\epsilon$ , can also fluctuate in time. In this work, we assume that the charge transfer primarily takes place via the adenine bases, which is justified since the ionization potential of thymine is  $\sim 0.7$  eV higher than that of

adenine.<sup>56</sup> In the simplest approximation, the values of  $\epsilon$  correspond to the ionization potential of the bases and the donor and acceptor. This simple picture holds for donor–DNA–acceptor systems in which only one positive charge has been generated. In the experimental results that we are considering here, the situations are somewhat more complicated since the injection of a positive charge from the photoexcited hole donor is accompanied by the formation of the anion **Sa**<sup>−</sup>.<sup>55,57</sup> Therefore, the electrostatic interaction between the positive charge on the bridge and the negative charge that remains on **Sa** has to be taken into account. The value of  $\epsilon_{ii}$  for a particular adenine site on the DNA bridge relative to the energy of the donor ( $\epsilon_{11}$ ) can be estimated using the following equation that is analogous to the Weller relation:<sup>58</sup>

$$\epsilon_{ii} = E_{\text{ion}}(\text{A}) - E_{\text{el.aff.}}(\text{Sa}) - E_{\text{exc}}(\text{Sa}) - E_{\text{elst}}(\text{A}^+\text{Sa}^-) - \Delta E_{\text{solv}} \quad (6)$$

In this equation,  $E_{\text{ion}}(\text{A})$  denotes the ionization potential of the adenine, while  $E_{\text{el.aff.}}(\text{Sa})$  and  $E_{\text{exc}}(\text{Sa})$  are the electron affinity and excitation energy of the stilbene **Sa**, respectively.  $E_{\text{elst}}$  denotes the electrostatic interaction between the positive and negative charge, and  $\Delta E_{\text{solv}}$  is the change in solvation energy upon charge separation. The latter two terms are discussed in more detail below. The sum of electron affinity of  $E_{\text{el.aff.}}(\text{Sa})$  and  $E_{\text{exc}}(\text{Sa})$  corresponds to the electron affinity of the excited state of **Sa**. The sum of the first three terms in eq 6 gives the energy needed to make a transition from the excited state of **Sa** to the pair of oppositely charged ions **Sa**<sup>−</sup>**A**<sup>+</sup> at infinite separation in vacuum. In reality, these charges are not at infinite distance in the DNA hairpins. Therefore, the (attractive) electrostatic interaction  $E_{\text{elst}}(\text{A}^+\text{Sa}^-)$  at their actual distance should be subtracted. Finally, the stabilization of the charge-separated pair by the solvent is likely to be more than for the neutral system (corresponding to the localization of the positive charge on the hole donor **Sa**). This difference in solvation energy,  $\Delta E_{\text{solv}}$ , therefore has to be taken into account in the values of  $\epsilon_{ii}$ .

The ionization potentials of the DNA bases in vacuum are well-established experimentally,<sup>56</sup> however, the hydrogen bonding will lower the ionization potential in the base pair. Hutter et al. estimated the ionization potential for an AT base pair in vacuum by using electronic structure calculations and found it to be equal to 8.04 eV.<sup>59</sup> In the DNA structure, the ionization potential will be lowered further by interactions between neighboring bases. On the basis of semiempirical calculations and DFT calculations, this reduction of the ionization potential was estimated to be  $\sim 0.7$  eV.<sup>45,46</sup> This results in an ionization potential for the adenine base when hydrogen bonded to thymine in the DNA stack of  $\sim 7.35$  eV. This value represents the average ionization potential, but dynamic fluctuations in the structure of the DNA will lead to fluctuations around this average. To gain insight in the amplitude and time scale of these fluctuations, we have calculated the energy of the HOMO in adenine for all snapshots obtained from the MD simulation described above. These calculations yielded a Gaussian distribution of site energies with a standard deviation of 0.15 eV. The fluctuations

(56) Hush, N. S.; Cheung, A. S. *Chem. Phys. Lett.* **1975**, *34*, 11–13.

(57) Lewis, F. D.; Wasielewski, M. R. Dynamics of photoinitiated hole and electron injection in duplex DNA. In *Charge transfer in DNA: From mechanism to application*, Wagenknecht, H.-A., Ed.; Wiley-VCH: Weinheim, Germany, 2005; pp 93–116.

(58) Weller, A. Z. *Phys. Chem. Neue Folge* **1982**, *133*, 93–98.

(59) Hutter, M.; Clark, T. J. *Am. Chem. Soc.* **1996**, *118*, 7574–7577.

in the site energy occur on a faster time scale than those in the charge transfer integrals. The details of these calculations are given in the Supporting Information. Note that although the fluctuations in the site energy are large they are still significantly smaller than the ionization potential differences between the bases (with the exception of adenine–guanine) so base pair sequence effect would still be observed experimentally.

The vacuum ionization potential of the **Sd** hole acceptor was calculated by DFT calculations and was found to be 6.68 eV. It is expected that the ionization potential in the DNA stack in solution will be lower by at least 0.5 eV, similar to the ionization potential of adenine. Calculations of the site energy of **Sd** for the 400 snapshots from the MD simulation on hairpin **2** resulted in a Gaussian distribution of orbital energies with a standard deviation of 0.17 eV, close to the width of the distribution obtained for the adenines.

The vacuum electron affinity of **Sa** was obtained from DFT calculations and found to be 1.08 eV. The excitation energy needed in eq 6 is known experimentally and equal to 3.35 eV.<sup>57</sup> This gives the sum of  $E_{\text{el.aff.}}(\text{Sa})$  and  $E_{\text{exc}}(\text{Sa})$  of 4.43 eV. The difference between this sum and the ionization potential of adenine in the DNA stack (7.35 eV) is 2.92 eV. Thus the formation of  $\text{Sa}^-$  and  $\text{A}^+$  at infinite separation in vacuum requires  $\sim 2.92$  eV.

In the hairpins considered here, the charges are not formed at infinite distance but still experience each other's electrostatic potential. Therefore, the electrostatic interaction between the positive and negative charge has to be included in calculations of the site energy. In order to obtain a realistic measure of the electrostatic interaction between the charges, we have calculated distributed sets of point charges for  $\text{Sa}^-$ ,  $\text{A}^+$ , and  $\text{Sd}^+$  by fitting them to the electrostatic potential obtained from Hartree–Fock calculations for the isolated  $\text{Sa}^-$ ,  $\text{A}^+$ , and  $\text{Sd}^+$ .<sup>60</sup> These point charges were used to calculate the electrostatic interaction between the  $\text{Sa}^-$  and  $\text{AT}^+$  ( $\text{Sd}^+$ ) at different positions along hairpin **6**. The distance dependence of the electrostatic interaction is shown in the Supporting Information. The interaction between  $\text{Sa}^-$  and a positive charge on the first AT base pair was found to be 2.38 eV. The electrostatic interactions discussed here were performed setting the dielectric constant equal to 1. The dielectric properties for DNA and the regions around it have been studied, and although no definite values were defined, these studies agree that the value inside the  $\pi$ -stack is small,  $\sim 2$ .<sup>61,62</sup> The calculations discussed below were not found to change qualitatively when realistic values for the dielectric constant inside the stack were used, although there are quantitative differences. Since we are mostly interested in the qualitative features, we have chosen to use  $\epsilon = 1$  to prevent the introduction of an additional unknown parameter.

Substituting  $E_{\text{ion}}(\text{A}) = 7.35$  eV,  $E_{\text{el.aff.}}(\text{Sa}) = 1.08$  eV,  $E_{\text{exc}}(\text{Sa}) = 3.35$  eV, and  $E_{\text{elst}}(\text{Sa}^- \text{A}^+) = 2.38$  eV in eq 6 and neglecting the solvation energy contribution ( $\Delta E_{\text{solv}}$ ) gives an estimate of the energy difference between the hole donor and the first bridge site of  $\sim 0.5$  eV. We expect that the solvation energy effect is relatively small, between 0.1 and 0.5 eV, since the surrounding water is excluded from the interior of the DNA and the first

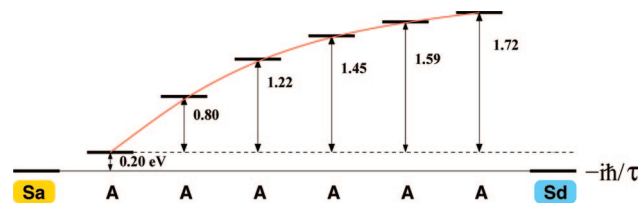


**Figure 3.** Schematic representation on the energetics of DNA hairpins. The red line indicates the Coulomb well from which the charge has to escape in order to move away from the hole donor.

layers of water are rigidly confined, resulting in a low effective dielectric constant.<sup>61–64</sup>

In the diagram in Figure 3, we have summarized the energetics of charge transfer in the DNA hairpins studied here. The energy gap between the donor and the first base is taken to be 0.2 eV, including a solvent stabilization of 0.3 eV (the average of 0.1 and 0.5 eV). Note that the uncertainty in this value is a few tenths of an electronvolt because of uncertainties in the estimates made above. For the farther bases, the energy increases gradually. The site energy for **Sd**,  $\epsilon_{NN}$ , is taken equal to  $\epsilon_{11}$ . In the experiment, this energy should be at least somewhat lower than the energy of the donor in order to provide a driving force for charge separation. In our simulation, the complex part added to  $\epsilon_{NN}$  ensures irreversible trapping at the acceptor.

We conclude from this analysis that the energy barrier for injection of a positive charge from the  $\text{Sa}^*$  into the first adenine in the hairpin is between 0 and 0.4 eV, which is relatively small. In order to move further away from **Sa**, a hole has to escape from the Coulomb well due to the electrostatic potential of  $\text{Sa}^-$ . Therefore, the site energies gradually increase as the charge moves toward the **Sd** hole acceptor. The energy of the fully charge-separated state  $\text{Sa}^-/\text{Sd}^+$  is slightly lower than that for the neutral excited state for hairpin **6**, leading to a small driving force for charge transfer. For shorter hairpins, this driving force is larger due to the higher electrostatic interaction between  $\text{Sa}^-$  and  $\text{Sd}^+$ .

**3. Charge Transfer Dynamics.** The energies and charge transfer integrals discussed in the preceding two sections can be used in eq 4 to set up the Hamiltonian for simulations of charge transfer in the DNA hairpins **1–6** (see Figure 1). We have taken the energy difference between the first two sites equal to 0.2 eV. Variation of this energy difference between 0 and 0.4 eV did not lead to qualitative changes in the results. The energy of the adenine bases along the stack was taken to increase gradually as shown in Figure 3. As discussed above, both the values of the site energies and the values of  $V^{\text{eff}}$  fluctuate in time. This is taken into account by adding a random fluctuation to the equilibrium values of  $V$  and  $\epsilon$ , sampled from a Gaussian distribution. The standard deviations and average values of  $V^{\text{eff}}$  of these distributions were taken from the calculations discussed above. The values of  $\epsilon$  and  $V^{\text{eff}}$  were taken to change after a time  $\Delta t$  that was sampled randomly from an exponential probability distribution  $P(t) \sim e^{-t/t_{\text{av}}}$  with an average time  $t_{\text{av}}$ . We estimated values of  $t_{\text{av}}$  for the fluctuations in  $\epsilon$  and  $V^{\text{eff}}$  of 0.1 and 0.5 ps, respectively, based on the data shown above and in the Supporting Information. Variation of  $t_{\text{av}}$  by a factor of 2 was not found to affect the calculated transfer kinetics.

(60) Cieplak, P.; Cornell, W. D.; Bayly, C. I.; Kollman, P. A. *J. Comput. Chem.* **1995**, *16*, 1357–1377.

(61) Yang, L.; Weerasinghe, S.; Smith, P. E.; Pettitt, B. M. *Biophys. J.* **1995**, *69*, 1519–1527.

(62) Young, M. A.; Jayaram, B.; Beveridge, D. L. *J. Phys. Chem. B* **1998**, *102*, 7666–7669.

(63) LeBard, D. N.; Lilichenko, M.; Matyushov, D. V.; Berlin, Y. A.; Ratner, M. A. *J. Phys. Chem. B* **2003**, *107*, 14509–14520.

(64) Siriwong, K.; Voityuk, A. A.; Newton, M. D.; Rosch, N. *J. Phys. Chem. B* **2003**, *107*, 2595–2601.

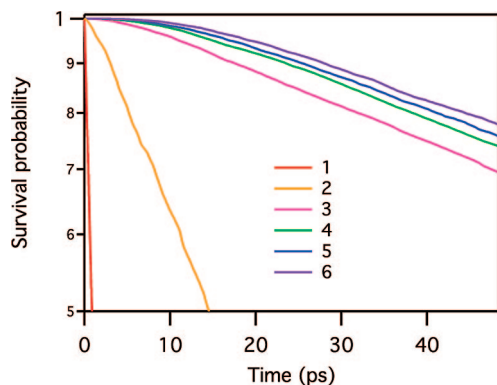


**Figure 4.** Calculated survival probability as a function of time for DNA hairpins 1–6.

**Table 1.** Calculated Rates for Hole Injection and Arrival for Hairpins 1–6

hairpin	hole injection $\times 10^{-10}$ $k_i$ ( $s^{-1}$ )	hole arrival $\times 10^{-10}$ $k_a$ ( $s^{-1}$ )
1	77	79.3
2	130	5.0
3	122	0.7
4	98	0.84
5	125	0.76
6	92	0.71

In Figure 4, the calculated survival probability of the charge is shown as a function of time for hairpins 1–6. The charge in hairpin 1 disappears very rapidly, and the decay is exponential in time. The decay for hairpin 2 is almost an order of magnitude slower but is still exponential in time. For hairpins 3–6, the decay is negligible at very short times, but at longer times, nearly exponential decay is observed. It appears that for these longer bridges it takes some time for the charge to move over the bridge before it arrives on the acceptor, whereas in hairpins 1 and 2, there is almost direct transfer from the donor to the acceptor. The rate constants for charge arrival,  $k_a$ , on the acceptor were obtained from exponential fits to the decay of the curves in Figure 4 at longer times. These rate constants are summarized in Table 1 and are plotted as a function of distance in Figure 5, together with the experimental data available for these hairpins. For hairpins 1–3, the calculated rate constant is found to decrease exponentially with distance with a  $\beta$  parameter of  $0.70 \text{ \AA}^{-1}$ . This value for  $\beta$  is very close to the value deduced from the experimental data by Lewis et al.,  $0.67 \text{ \AA}^{-1}$ .<sup>26</sup> The good

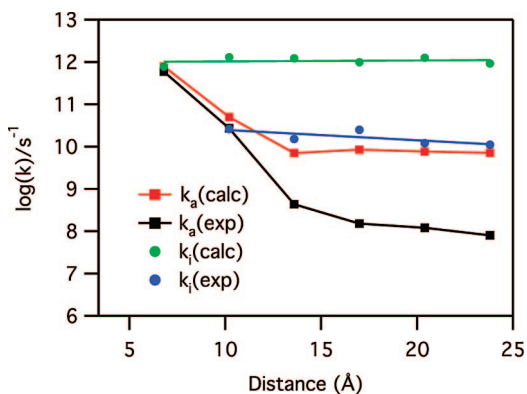


**Figure 5.** Calculated rate constants for charge injection ( $k_i$ ) and charge arrival ( $k_a$ ) plotted against the distance between donor and acceptor. The experimental data of Lewis et al.<sup>25,26</sup> are included for comparison.

correspondence with the experimental data for hairpins 1 and 2 is also evident from Figure 5, which shows that the values of the calculated rates are very close to the experimental ones. For hairpins containing more than 3 AT base pairs,  $k_a$  is essentially independent of the distance between the donor and acceptor.

This is also consistent with experimental results, although the calculated values of the arrival and injection rate constants for hairpins 4–6 are 2 orders of magnitude higher than those obtained from experiment. We attribute this difference to absence of geometry relaxation in the present model. This energy relaxation can occur in both the intramolecular degrees of freedom and in the surrounding solvent. The intramolecular energy lowering by such relaxation when a charge is localized on a single base can be estimated by comparing the vertical and adiabatic ionization potential of the isolated bases. Experiments and electronic structure calculations show that the difference between these values is 0.18 (experiment) and 0.36 eV (MP2 calculation) for an isolated adenine.<sup>56,65</sup> Depending on the strength of the coupling between the charge and the nuclear degrees of freedom, geometry relaxation can lead to temporal localization of the charge and to polaronic effects.<sup>34,35</sup> These effects are expected to lead to slower migration of charges since the presence of the relaxation leads to a local lowering of the site energy, which impedes further migration of the charge. Previously, the crossover from weak to strong distance dependence has also been attributed to the (distance dependent) reorganization energy. This effect still plays a role here, leading to somewhat stronger distance dependence for short sequences and lower transfer rates for longer bridges.<sup>63</sup>

On the basis of their experimental data, Lewis et al. attributed the change from an exponential distance dependence for short hairpins to almost distance-independent transfer in longer hairpins to a crossover from a single-step superexchange to a hopping mechanism.<sup>23,26</sup> This implies that for short AT bridges the amount of charge on the bridge is always negligible since the charge essentially transfers to the acceptor in a single step, whereas for the longer bridges, a considerable amount of charge builds up on the bridge. Moreover, it was shown in the experiments by Lewis et al. that the rate at which the positive charge disappears from the donor site, the injection rate, is essentially independent of the number of AT base pairs in the bridge.<sup>25,26</sup> For hairpins 1 and 2, the experiments show that the rate constant for charge injection is the same as the rate constant for arrival at the hole acceptor, indicating that the charge transfer indeed occurs in a single step. In the case of the longer bridges, the rate constant for charge injection was considerably faster than that for hole arrival, suggesting a significant charge density on the AT bridge during transfer.

A more detailed insight into the mechanism by which charge migrates from **Sa** to **Sd** through the AT bridge in the DNA hairpins considered here can be obtained by examining how the charge density on the donor and bridge sites evolves in time. In Figure 6, the amount of charge that is present on the hole donor, the bridge, and the complete hairpin is plotted as a function of time for hairpins 1, 2, and 6. The population of charge on a certain site  $i$  simply corresponds to the square of the coefficient of the wave function for that site. Therefore, the population on the donor site at time  $t$  is equal to  $c_1^2(t)$ , and the population on the bridge is  $\sum_{n=2}^{N-1} c_n^2(t)$ . The full population is equal to the survival probability defined in eq 5.

(65) Olofson, J.; Larsson, S. *J. Phys. Chem. B* **2001**, *105*, 10398–10406.



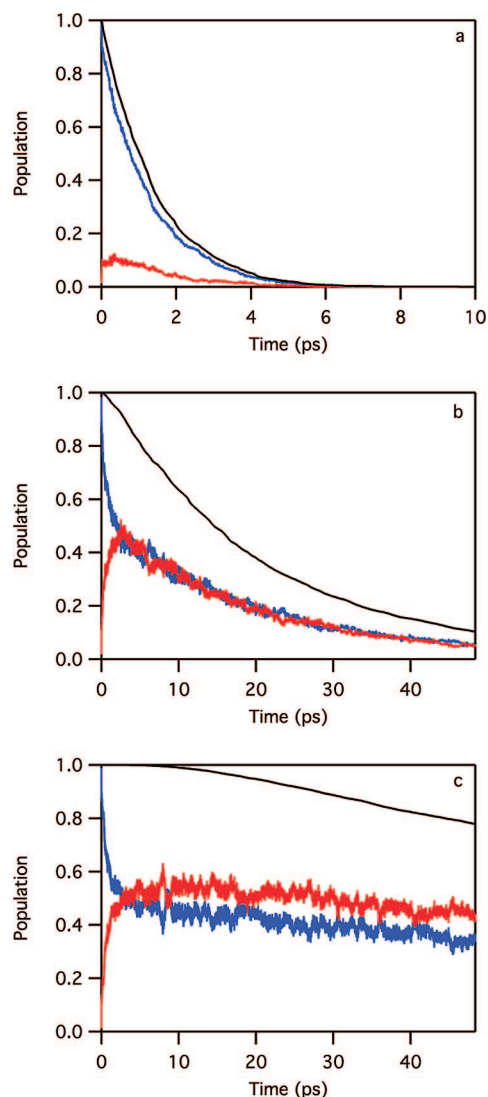


**Figure 6.** Population as a function of time for hairpins **1** (a), **2** (b), and **6** (c). Black: full population, blue: population on donor, red: sum of populations on all bridge sites.

For hairpin **1**, a very small population of charge builds up on the bridge during charge transfer. When the decay of the population on the donor site and that of the full population are compared, it becomes clear that the transfer is essentially a single-step process; the decay of these two curves is almost the same.

For hairpin **2**, a different picture emerges. During the first few picoseconds, almost half of the charge population moves to the DNA bridge. After this initial stage, the charge slowly decays with almost equal rate from the donor and the bridge. When the decay curves for the donor and the bridge are normalized for the total amount of charge present at time  $t$ , it is found that the relative amount of charge on the bridge stays constant after the initial spreading of the charge onto the bridge.

In Figure 6c, the populations are shown for hairpin **6**. The initial stage of the charge transfer in this case is similar to that found for hairpin **2**; the charge rapidly spreads out from the donor onto the bridge. After this fast spreading, the charge disappears very slowly from both the donor and the bridge with the same rate. The relative amount of charge on the bridge is somewhat larger than on the donor in this case.

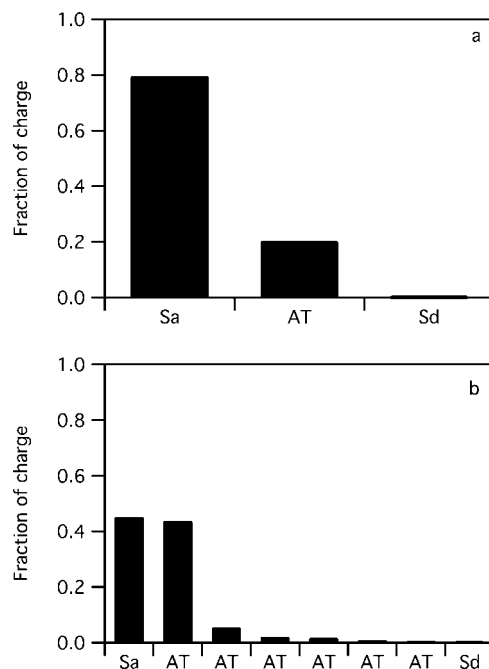


**Figure 7.** Distribution of charge on hairpin **1** (a, after 1 ps) and **6** (b, after 50 ps) normalized to the total amount of charge present.

The initial fast decay of the charge on the donor site is close to exponential, and we have made fits to these curves in order to obtain a value for the rate of injection ( $k_i$ ) of charge into the bridge. The values obtained are listed in Table 1 and plotted in Figure 5 for the different hairpins. The rate of charge injection is found to be independent of the donor–acceptor distance. The independence of  $k_i$  of the hairpin length is in agreement with the experimental data of Lewis et al.,<sup>25,26</sup> although the absolute value of the injection rate we calculate here is 2 orders of magnitude higher than that in the experimental data. A possible source of this difference can be the neglect of geometry relaxation as discussed above. Relaxation of the **Sa** excited state will lead to an increase in the injection energy and, hence, to a lower rate. Calculations using an injection energy of 0.6 eV (instead of 0.2 eV) give an injection rate that is 1 order of magnitude smaller, which supports this explanation.

The data in Figure 6 clearly show that for longer DNA hairpins a considerable charge density builds up on the bridge. The actual distribution of the charge in the hairpin systems is described by the square of the wave function in eq 2. The charge distribution for hairpins **1** and **6** during the charge transfer process is shown in Figure 7. In hairpin **1**, most of the charge is on the **Sa** donor. While some charge density builds up on the (single) AT bridge site, the charge rapidly moves further to the **Sd** acceptor where it instantaneously disappears. This is consistent with the data in Figure 6a, which show that the population essentially decays by direct charge transfer from **Sa** to **Sd**.

For hairpin **6** (Figure 6c), an appreciable amount of charge builds up on the bridge. The charge distribution in Figure 7 shows that the majority of the charge on the bridge is located on the first adenine. This is not surprising considering the site's energies along the AT stack (see Figure 3). The average site energy of the first adenine is only 0.2 eV higher than that of the **Sa**. Although the average site energy of the first adenine is much larger than the average charge transfer integral (close to zero), the fluctuations in the site energies and in the charge

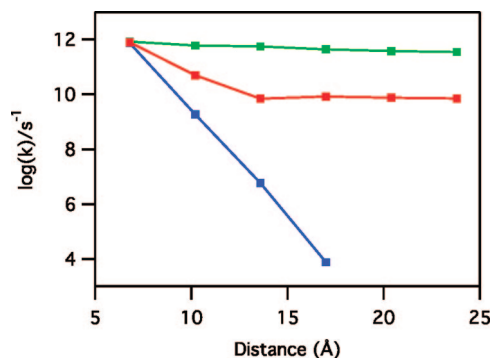


**Figure 8.** Calculated rate constants for charge arrival at the acceptor as a function of distance. Blue: including only the electrostatic interactions (no fluctuations in  $\epsilon$  and  $J$ ), green: only fluctuations in  $\epsilon$  and  $J$ , and red: including both electrostatic interaction and fluctuations in  $\epsilon$  and  $J$ .

transfer integral are sufficiently large that the charge can populate this site.

For the second adenine, the energy relative to the **Sa** increases to almost 1 eV, making the probability of finding the charge here much smaller. Once the charge is uniformly distributed over the **Sa** and the first adenine on the bridge, the transfer of charge slows down since the charge has to overcome the barrier presented by the other adenines. This barrier is mostly due the electrostatic interaction between the hole and the negative charge on **Sa**.

**4. Effects of Electrostatic Interaction and Structural Fluctuations.** In the calculations described above, we include two important factors that are missing in almost all earlier discussions:<sup>2,3,14,35</sup> the electrostatic interaction between the hole on the hairpin and the negative charge on the **Sa** donor, and the effect of structural fluctuations. In order to gain more insight in the separate effects of these factors, we have performed additional simulations including only one of the two. We have performed a series of charge transfer calculations exactly as described above but without including fluctuations in the site energies and charge transfer integrals. All site energies were fixed on their equilibrium values (including the Coulomb well). The charge transfer integrals were all taken equal to 0.05 eV, the equilibrium value of  $J^{\text{eff}}$  between two neighboring adenines. In Figure 8, the rates of charge arrival at the acceptor obtained from these simulations are plotted as a function of the distance between **Sa** and **Sd**. The value of  $k_a$  exhibits a strong exponential dependence on distance with a  $\beta$  value (see eq 1) equal to  $1.8 \text{ \AA}^{-1}$ . No crossover to a regime with a weak dependence on distance was found in these calculations. The distance dependence found here is much stronger than found above for hairpins 1–3 ( $\beta = 0.70 \text{ \AA}^{-1}$ ), which shows that the absence of geometry fluctuations dramatically changes the results. The absence of structural fluctuations can be achieved experimentally by studying frozen solutions. For such experiments, our simulations predict a strong distance dependence and no occurrence of a plateau value for the charge transfer rate for longer bridges.

Figure 8 also includes the values for  $k_a$  obtained from calculations where only geometry fluctuations are considered. All the site energies of the AT bridge were set equal to a value 0.2 eV higher than that of the **Sa** donor (indicated by the dashed line in Figure 9), and fluctuations in the site energies and charge transfer integrals are described in the same way as discussed above. In this case, the distance dependence is very weak even for the shortest few hairpins. If an exponential dependence on distance is assumed, a  $\beta$  value of  $0.05 \text{ \AA}^{-1}$  is obtained. This

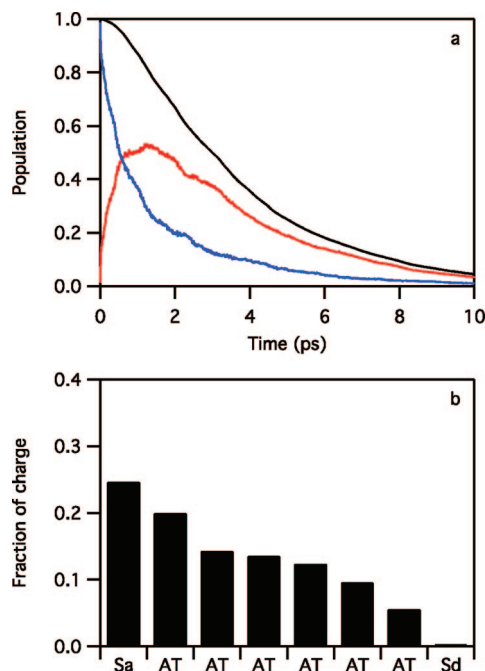


**Figure 9.** (a) Evolution of the amount of charge present on **Sa** (blue), the DNA bridge (red), and the total population (black) with time for hairpin **6**. (b) Distribution of charge on hairpin **6** during the hole transfer (after 3 ps) normalized to the total amount of charge present at  $t = 3$  ps. All site energies were set equal to 0.2 eV.

unrealistic  $\beta$  value suggests that a hole moves from the donor to the acceptor by a fluctuation-assisted incoherent mechanism. Even though the average value of the site energy difference between **Sa** and the AT base pairs on the bridge is large compared to the charge transfer integrals, the fluctuations in these site energies and charge transfer integrals are sufficiently large for the charge to acquire enough energy to migrate onto the bridge. This is evident from the populations plotted in Figure 9a. After  $\sim 1$  ps, the majority of the charge density is on the bridge. As can be seen in Figure 9b, the distribution of charge along the stack of AT base pairs is almost uniform, in contrast to the results in Figure 7. It should be noted that if the geometry of the bases would be allowed to react to the presence of the charge this would lead to a localized charge on the bridge at a certain time.

## Summary and Conclusions

In this paper, we present an extensive study of the effects of structural fluctuations and electrostatic interactions on the rates of photoinduced charge transfer in stilbene-capped DNA hairpins consisting only of adenine–thymine base pairs. The effect of structural fluctuations was studied by molecular dynamics simulations combined with density functional theory calculations of charge transfer integrals and site energies. We find that the fluctuations in the charge transfer integrals are of the same order of magnitude or larger than their equilibrium values. The fluctuations found in the site energies, the energy of a charge localized on a single subunit, are also found to be relatively large. The distributions of the charge transfer integrals and site energies were shown to be Gaussian with standard deviations close to 0.05 and 0.15 eV, respectively.

The charge transfer integrals and site energies were used in tight-binding calculations of the dynamics of charge transfer in a series of DNA hairpins of increasing length. We show that

when fluctuating charge transfer integrals and site energies are used, together with a fairly accurate description of the electrostatic interaction between the positive charge on the AT bridge and the negative charge on the hole donor, good qualitative agreement with experimental data is obtained. For the shortest three hairpins containing 1–3 adenine–thymine base pairs between the donor and the acceptor, an exponential distance dependence of the charge transfer rate is obtained. For longer adenine–thymine bridges, almost no distance dependence was found from these calculations. The simulations indicate that the strong distance dependence for the shorter hairpins is largely due to the increasing effective barrier height between the donor and the acceptor. This barrier is caused by the electrostatic interaction between the hole and the negative charge on the hole donor. After the first three AT base pairs, this effective barrier changes only weakly and the charge transport is mostly dominated by fluctuation-assisted incoherent charge migration along the adenine–thymine bridge.

Our calculations show that the rate at which the charge moves away from the hole donor, the injection rate, is almost independent of the length of the AT bridge, in qualitative agreement with experimental data for hairpins **3–6**. This indicates that in these hairpins the charge migrates to the bridge before it arrives on the acceptor, thus suggesting that the charge transfer does not occur by single-step tunneling. Analysis of

the charge distribution on the bridge during charge transport shows that most of the charge on the bridge is located on the first adenine adjacent to the hole donor. The charge density on the other adenines is very small because the site energies are much higher here due to the weaker electrostatic interaction with the negative charge on the hole donor.

**Acknowledgment.** This work supported by the Dutch Foundation of Scientific Research (NWO) through an NWO-VENI grant to F.C.G. The National Science Foundation (NSF) is acknowledged for financial support (CHE-0628130 to GCS). M.R. and Y.B. thank the Chemistry Divisions of the NSF and ONR for financial support. S.T. acknowledges PNNL for supercomputing time. M. McCullagh is acknowledged for assistance in setting up the MD simulations. F.D. Lewis is acknowledged for stimulating discussions.

**Supporting Information Available:** Detailed information on the molecular dynamics simulations, detailed information on (fluctuations in) the charge transfer integrals and site energies, and coordinates for the optimized structures used for the calculations. This material is available free of charge via the Internet at <http://pubs.acs.org>.

JA078162J